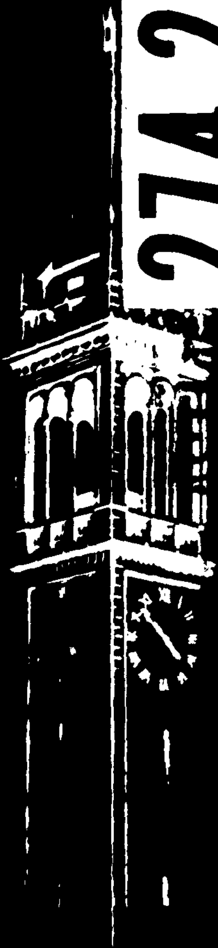

Determination of Physical Parameters of Drift Transistors Having a Diffused Collector Junction

by

A. R. Boothroyd

Series No. 60, Issue No. 391
AF 49(638)-1043
August 11, 1961

ELECTRONICS RESEARCH LABORATORY

UNIVERSITY OF CALIFORNIA
BERKELEY CALIFORNIA

AFOSR 2118

Electronics Research Laboratory
University of California
Berkeley, California

DETERMINATION OF PHYSICAL PARAMETERS OF DRIFT TRANSISTORS HAVING A DIFFUSED COLLECTOR JUNCTION

by

A. R. Boothroyd

Institute of Engineering Research
Series No. 60, Issue No. 391

Air Force Office of Scientific Research
of the Air Research and Development Command;
Department of the Navy, Office of Naval Research;
and Department of the Army
Contract No. AF 49(638)-1043

August 11, 1961

LIST OF PRINCIPAL SYMBOLS

N	impurity density in the base
L	critical length defining an exponential distribution of N
D	diffusion constant of minority carriers in the base
m	electric field parameter $= \Delta V/(kT/q) \doteq w/L$
w	electrical base width
d	collector depletion layer width
A_e	emitter area
K	absolute permittivity of base material
ψ_{eo}	contact potential of emitter junction
n_i	intrinsic hole and electron density
w_b	distance between collector and emitter junction transition points
τ	intrinsic base transit time
τ'	"effective transit time" $= 1/(2\pi f_T)$

SUMMARY

A procedure for the determination of physical parameters of drift transistors with a diffused collector junction has been developed on the assumption of a device model with exponential base grading. Only relatively low-frequency measurements are involved. Studies have been made of a double-diffused silicon mesa unit (Fairchild 2N696) and the results obtained suggest that the theory used may be adequate for practical application, despite discrepancies between the assumed model and the actual device. Good correlation between certain known design values of physical parameters of the device, and the values deduced from measurements, has been obtained. More investigation is necessary, however, in order to establish the conditions of validity, accuracy and possible need for further elaboration of the approach presented.

TABLE OF CONTENTS

LIST OF ILLUSTRATIONS

I. INTRODUCTION

It has been found possible to derive a considerable amount of physical data for drift transistors of alloy-junction type by measuring the dependence of effective transit time (i.e., $1/\omega_T$) and collector capacitance on collector voltage[1, 2]. Assuming a specific form of impurity density distribution in the base--viz. exponential or complementary error function--such measurements lead to the derivation of base width, field parameter $m = \Delta Vq/kT$, collector depletion layer width, emitter area, impurity density as a function of distance and other related properties. The physical properties exploited in these derivations are illustrated in Figure 1a: a change in collector voltage causes change in both the minority carrier charge Q in the base region and the space charge in the collector depletion layer, resulting in corresponding changes in base transit time $\tau = Q/I_e$ and collector capacitance C_c. In the case of the alloy junction device, as shown, the changes in base width and depletion layer thickness are equal and opposite, a property that leads to relatively simple relationships between changes in τ and C_c. Specifically, for an alloy junction transistor with base impurity density distribution of the form

$$N = N_o e^{-x/L}, \qquad (1)$$

it may be shown that

$$L \simeq \sqrt{\frac{D(\tau_1 - \tau_2)}{\ln\left(\frac{V_{c1}}{V_{c2}}\frac{C_{c1}}{C_{c2}}\right)}} \qquad (2)$$

where τ_1, C_{c1} and τ_2, C_{c2} are measured at collector voltages V_{c1} and V_{c2}, respectively. Then, for given V_c,

$$\tau \simeq \frac{L^2}{D}(m - 1) \qquad (3)$$

so that if $m \geq 3$

$$m \simeq \frac{\tau D}{L^2} + 1 \qquad (4)$$

and base width w is

$$w \simeq m\,L \qquad (5)$$

Having determined the above parameters, the values of impurity density N_o and emitter area follow from measurements of the dependence of emitter depletion capacitance on reverse bias voltage and the d.c. $I_c \sim V_{eb}$ characteristic of the device with emitter forward and collector reverse biased.

The above process of parameter evaluation is applicable only for a device with a step collector junction and exponential base impurity grading. If the collector junction is graded, as when formed by a diffusion process (e.g., mesa device), changes in base width and collector depletion layer width resulting from collector voltage change are not equal and opposite, as illustrated in Figure 1b: equation (2) does not apply in such a situation. This report presents a procedure for the derivation of physical parameters of drift transistors of diffused collector junction type, following along the lines outlined above for the step junction device. Exponential base grading is assumed, so that equations (3) - (5) apply. Alternatively, a complementary error function distribution of impurity density may be considered and similar relationships derived, equations (3) and (4) still being valid[2]. The most appropriate form of base grading needs to be established for the class of device concerned, possibly using the approach presented in reference 2; this matter is not pursued, however, in the present report.

II. THEORETICAL BASIS OF THE METHOD OF PHYSICAL PARAMETER DERIVATION

In order to keep the analysis within reasonable bounds of simplicity it is necessary to represent the transistor by a somewhat idealized model, as follows. The device cross-section of Figure 2a is assumed, for a mesa or planar diffused base device of linear or circular geometry. All injected minority carriers comprising collector current are supposed to flow directly from emitter to collector within the emitter area A_e, without side effects.

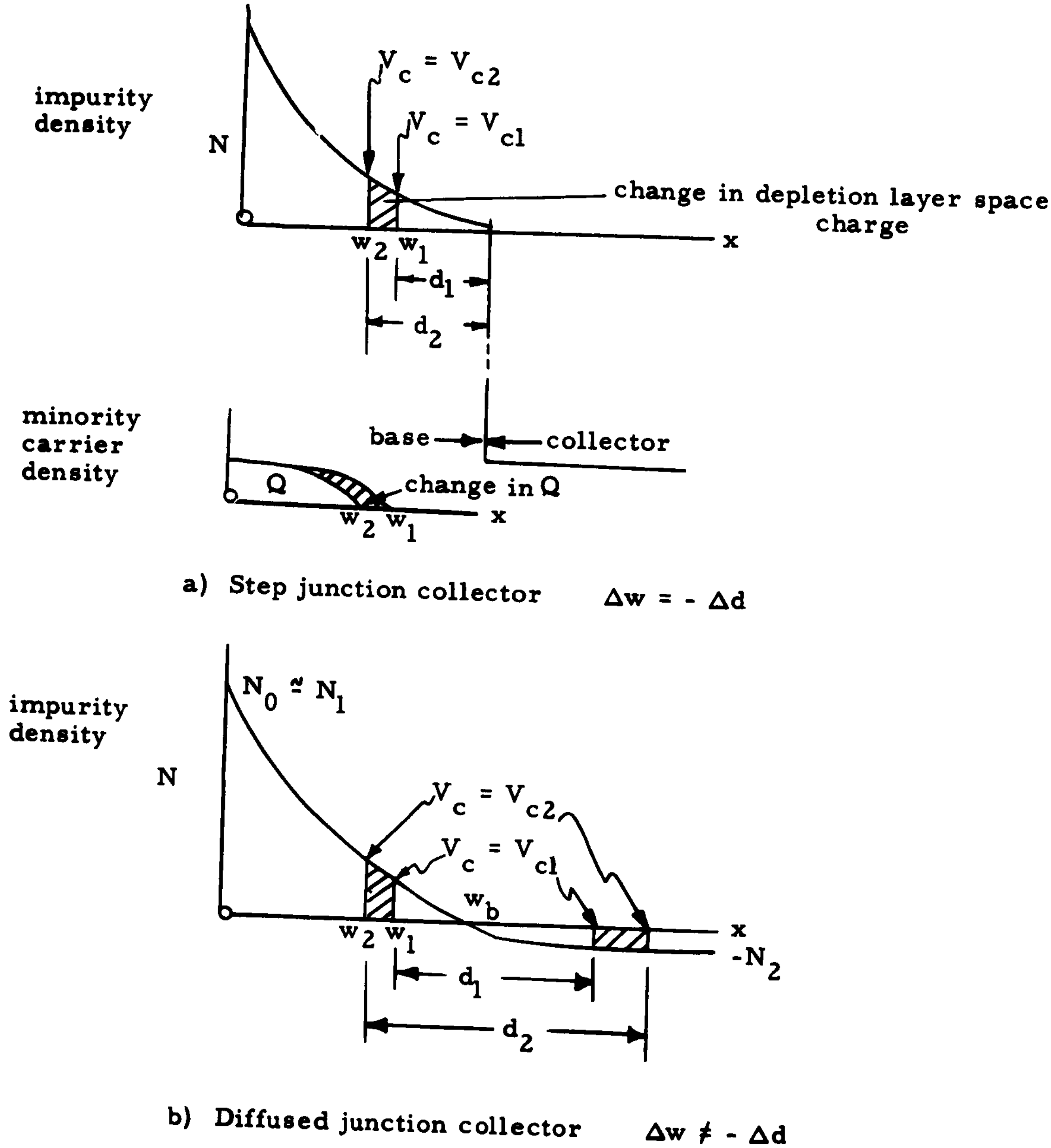

Figure 1. Step and Graded Collector Junctions

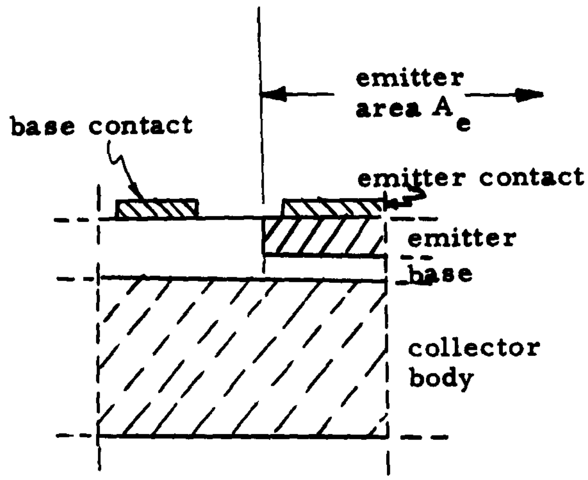

a) Assumed device cross-section

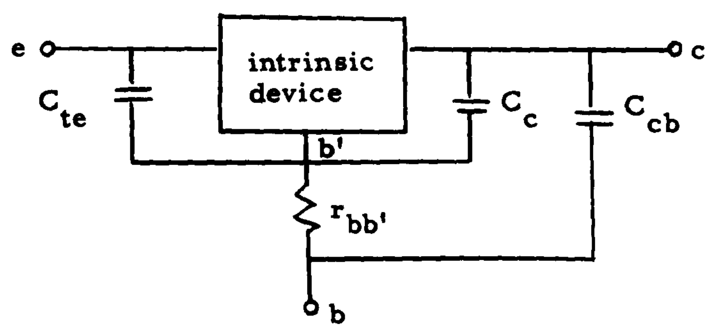

b) Assumed form of equivalent circuit (representation of collector body resistance omitted)

Figure 2. Device Assumptions

The effective base region is thus of area A_e and width w, and is regarded as obeying ideal one-dimensional theory. The complete device is considered to be represented by the equivalent circuit of Figure 2b in which C_c is the part of the total collector depletion capacitance opposite the emitter area A_e.

Further assumptions are that the base impurity density is (see Figure 1b) of the form

$$N(x) = N_1 \; e^{-x/L} - N_2, \tag{6}$$

so defining the graded collector junction transition point at

$$x = w_b = L \ln \, (N_1/N_2), \tag{7}$$

and that the emitter junction is either of step or very abrupt graded transition.

II.1 <u>Evaluation of the Basic Parameters L, m and w</u>

The property utilized as the starting point in the determination of physical parameters is that the total depletion layer space charge is zero. Thus assuming complete depletion of impurities within depletion layer thickness d, and zero depletion elsewhere,

$$\int_{w}^{w+d} N(x) \, dx = 0 \tag{8}$$

giving the relationship

$$e^{w/L} = \frac{N_1}{N_2} \cdot \frac{L}{d} \left(1 - e^{-d/L}\right) = e^{m} \tag{9}$$

Taking now two values V_{c1}, V_{c2} of collector reverse voltage,

$$\begin{aligned} e^{\left(w_1 - w_2\right)/L} = e^{m_1 - m_2} &= \frac{d_2}{d_1} \cdot \left(\frac{1 - e^{-d_1/L}}{1 - e^{-d_2/L}}\right) \\ &= \frac{d_2}{d_1} \cdot \frac{1}{F} \end{aligned} \tag{10}$$

Now if $d_1, d_2 >> L$, $F \simeq 1$ and

$$e^{m_1 - m_2} \simeq \frac{d_2}{d_1} = \frac{C_{c1}}{C_{c2}} \tag{11}$$

The assumption that $\frac{d}{L} >> 1$ will be made at this stage, but is not essential; if this condition is not obeyed the effect of the factor F may be included, as shown later. It should be noted that d/L does not need to be very large for $F \simeq 1$ because of the exponentials involved.

Writing m in terms of base transit time τ from equation (3), one gets

$$\tau_1 - \tau_2 \simeq \frac{L^2}{D} \cdot \ln (C_{c1}/C_{c2}) \tag{12}$$

where τ_1, C_{c1} and τ_2, C_{c2} are for collector voltages V_{c1} and V_{c2}, respectively. If now V_{c2} is fixed and V_{c1} varied, plotting $\tau_1 - \tau_2$ against $\ln (C_{c1}/C_{c2})$ should give a straight line, so verifying applicability of the theory for a given device and yielding the value of L from the slope of the line. Alternatively, for two collector voltages,

$$L \simeq \sqrt{\frac{D\,(\tau_1 - \tau_2)}{\ln (C_{c1}/C_{c2})}} \tag{13}$$

If $d/L \not\gg 1$, then from equation (10)

$$L = \sqrt{\frac{D\,(\tau_1 - \tau_2)}{\ln (C_{c1}/F\,C_{c2})}} \tag{14}$$

where F involves knowledge of L, d_1 and d_2. Equation (14) may be solved for L by iteration if d is separately determined, as discussed below.

Having evaluated the critical length L, m and w follow from equations (4) and (5), repeated here:

$$\left.\begin{aligned} m &= \frac{\tau D}{L^2} + 1 \\ w &= m\,L \end{aligned}\right\} \tag{15}$$

II. 2 Evaluation of Other Parameters

The emitter area A_e, collector depletion layer width d and impurity densities N_1, N_2 may be evaluated if additional measurements are carried out.

For a step emitter junction of an n-p-n device, the depletion capacitance

$$C_{te} \simeq A_e \left[\frac{q \, K N_1}{2(\psi_e)}\right]^{1/2} \tag{16}$$

where

$$\psi_e = \psi_{eo} + V_{eb}$$

and the impurity density in the emitter depletion layer region of base material $\simeq N_1$. Plotting $1/C_{te}^2$ against reverse V_{eb}, a straight line of slope $K_1 = 2/(q \, K \, N_1 \, A_e^2)$ results for such a junction from which the value of $N_1 \, A_e^2$ is known; viz.

$$N_1 \, A_e^2 = 2/(q \, K \, K_1) \tag{17}$$

For small emitter current, such that true low level injection conditions obtain, and with the collector junction reverse biased,

$$I_c \simeq A_e \frac{n_i^2}{N_1} \cdot q \frac{D}{L} e^{-qV_{eb}/kT} + I_o \tag{18}$$

for an n-p-n device. Voltage drop across $r_{bb'}$ is assumed to be negligible so that V_{eb} is the voltage applied across the emitter junction. Plotting I_c against $\exp(- qV_{eb}/kT)$ gives a straight line of slope K_2 where

$$\frac{A_e}{N_1} = K_2 \cdot \frac{L}{n_i^2 \, q \, D} \tag{18}$$

Hence, from equations (17) and (18),

$$A_e = \left[\frac{2\,K_2\,L}{q^2\,\kappa\,K_1\,n_i^2\,D}\right]^{1/3} \tag{19}$$

$$N_1 = \frac{A_e\,n_i^2\,q\,D}{K_2\,L} \tag{20}$$

N_2 follows from equation (9), viz.

$$N_2 = N_1 \cdot \frac{L}{d}\left(1 - e^{-d/L}\right) e^{-m}, \tag{21}$$

provided that d is known. The distance w_b between emitter and collector junctions is also defined by the ratio N_1/N_2 as in equation (7).

Knowledge of the "inner" collector capacitance C_c allows the value of d to be calculated, assuming this capacitance to represent area A_e of the collector depletion layer, since then

$$C_c = \frac{\kappa\,A_e}{d}. \tag{22}$$

Measurement of $r_{bb'}$ and the product $r_{bb'}\,C_c$ give the value of C_c.

II. 3 Iteration

After carrying through the above sequence of calculations based on the condition $F \approx 1$, it is necessary to verify that this assumption is valid. If d/L is not sufficiently large for $F \approx 1$, as may be the case for a practical device, the value of L may be determined by iteration. Using the F value calculated as above, equation (14) is used to obtain a modified value of L. A_e is then recalculated from equation (19), d from (22) and a new F value obtained. This process is iterated until a further step leads to no further change in L.

III. MEASUREMENT TECHNIQUES

For the above process of parameter determination to be carried out, the following quantities need to be measured:

1. base transit time τ
2. collector capacitance ratio C_{c1}/C_{c2} for two collector voltages
3. emitter depletion capacitance C_{te}
4. $I_c \sim V_{eb}$ characteristic
5. extrinsic base resistance $r_{bb'}$.

III.1 Base Transit Time Measurements

It is required to determine τ and also transit time differences for two collector reverse bias voltages; in the latter very small fractional differences are possibly involved. For this purpose the bridge arrangement of Figure 3 may be used.

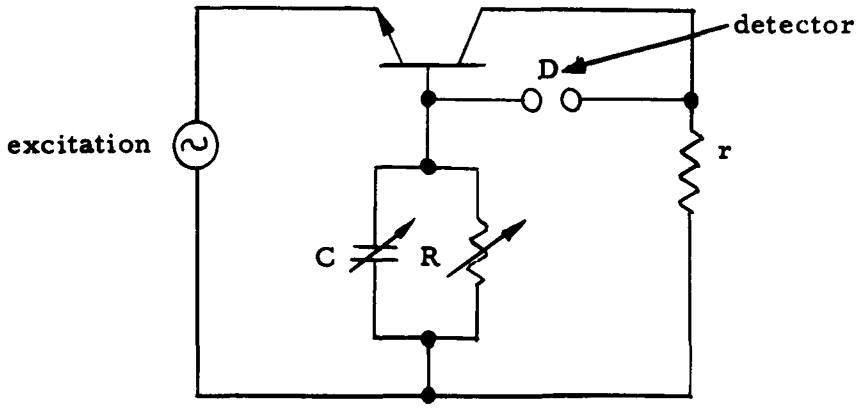

Figure 3. Arrangement of Bridge for Measurement of Transit Time

The bridge balance conditions are as follows: with R, C adjusted for null indication by the detector the transistor is operating with collector effectively shorted to base; thus

$$\frac{i_c}{i_b} = \beta = \frac{R}{r\,(1 + j\omega CR)} = \frac{\beta_o}{1 + j\omega/\omega_\beta} \tag{23}$$

so that

$$\left.\begin{aligned} \beta_o &= R/r \\ \omega_\beta &= 1/CR \\ \text{and} \quad 1/\omega_T &= Cr = \tau' \end{aligned}\right\} \quad \text{if} \quad \beta_o >> 1 \tag{24}$$

Now $\quad \tau' = \tau + C_{te}\, r_d$ + $\quad$ (25)

where τ is the base transit time Q/I_e and

$$r_d = kT/q\, I_e$$

Plotting $\tau' = 1/\omega_T$ against $1/I_e$ yields a straight line of slope $C_{te} \cdot kT/q$; extrapolating to $1/I_e = 0$ gives τ.

The bridge is convenient for measuring transit time differences since

$$\tau_1 - \tau_2 = \tau_1' - \tau_2' = r\,(C_1 - C_2) \tag{26}$$

Details of the practical arrangement of the bridge used for the measurements reported in Section IV are given in Appendix I. A noteworthy feature is the incorporation of a variable capacitor of small range calibrated directly in terms of $C_1 - C_2$ for facilitating transit time difference measurements.

+Assuming collector capacitance effects to be negligible. Otherwise $\quad \tau' \approx \tau + (C_{te} + C_c + C_{cb})\, r_d \quad$ (25a)
if effects of collector body resistance may be neglected (i.e., this resistance on I_e sufficiently small for "Miller effects" to be insignificant). Referring to Figure 2b, presence of $r_{bb'}$ is ignored in arriving at equation (25a).

III. 2 Measurement of Collector Capacitance Ratios

With a base cross-section as in Figure 2a, it would seem reasonable to employ the ratio of either C_c values, or of total collector capacitance

$$C_{ob} = C_c + C_{cb'}$$

in equations (12) to (14), provided that stray capacitance external to the collector depletion layer is negligible. In cases where stray capacitance is an appreciable fraction of C_{ob}, C_c ratios must be used.

In practice it is more convenient to evaluate C_{c1}/C_{c2} as the ratio of $r_{bb'} C_c$ products for the collector voltage concerned, this product being readily measurable. Perhaps the most satisfactory method of determining $r_{bb'} C_c$ is by means of the Turner bridge[3]. In the absence of such a bridge an alternative method is to use the Wayne Kerr admittance bridge in the manner of Figure 4.

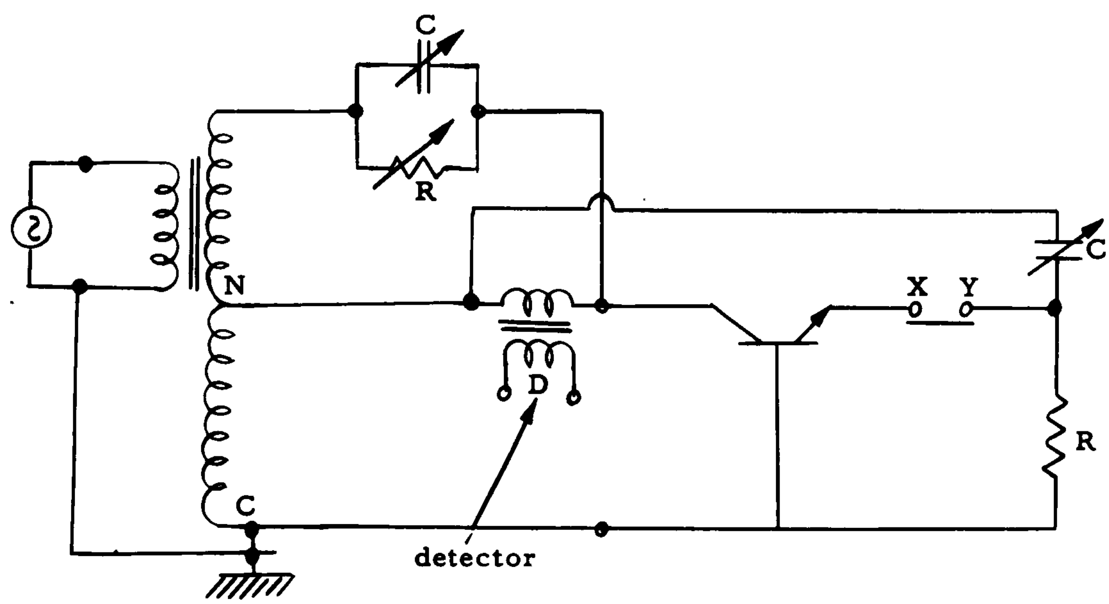

Figure 4. Arrangement for Measurement of $r_{bb'}C_c$ Using Wayne Kerr Bridge

With the points XY unconnected the bridge is balanced and C_{ob} (i.e., the common base parameter h_{22}) measured. XY are then connected together and C is adjusted so that the bridge is again balanced; then

$$CR = r_{bb'} C_c \tag{27}$$

This method was used for the measurements of the next section, the practical arrangement of the bridge being as in Appendix II. The same jig was used for measurement of C_{te} as a function of reverse V_{eb}, by interchanging the emitter and collector connections.

III. 3 Measurement of $r_{bb'}$

There are many possible methods of measuring extrinsic base resistance values[4], though the significance of the results obtained is often difficult to interpret in view of the distributed nature of extrinsic base region effects. For the present purpose it is preferable to use methods of measurement that are as closely as possible under the same conditions of operation of the transistor as employed when determining the product $r_{bb'} C_c$. Thus the transistor should be operated under the same d.c. bias conditions and at the same order of frequency, so that the flow of base current originates uniformly over the base cross-section as in the measurement of τ'.

The method employed was to measure the base input y_{11} parameter with emitter common, at a frequency of the order of f_β (actually the same as for the τ' measurement), and to evaluate $r_{bb'}$ from a knowledge or estimate of all other relevant equivalent circuit parameters involved in this admittance. Thus, an estimate is made of C_{cb}, having measured C_{ob}; then if effects of collector body resistance are negligible

$$\left.\begin{array}{l} y_{11}' = y_{11} - j\omega C_{cb} \\ \text{where} \\ 1/y_{11}' = r_{bb'} + 1/y_{b'e} \end{array}\right\} \tag{28}$$

From measurements made at the same bias point and frequency with the bridge of Section III.1

$$y_{b'e} \approx (1 - \alpha_o)/r_d + j\omega(\tau'/r_d - C_{cb})^{+} \tag{29}$$

+See footnote on page 10 in regard to the approximation involved in this expression.

with appropriate choice of frequency the difference of real parts of $1/y_{11}'$ and $1/y_{b'e}$ gives $r_{bb'}$ with reasonable accuracy. Having carried through the full procedure of calculation of Section II, the initial estimate of C_{cb} may be checked and if necessary corrected.

IV. PRACTICAL RESULTS

The measurements outlined in the previous section have been carried out for a variety of transistors of diffused base type having f_T ranging between 50 mc/s and 700 mc/s; the results obtained indicate that the measurement techniques described are suitable for the practical application of the parameter derivation process. For detailed study, an n-p-n silicon mesa transistor, Fairchild Type 2N696, was chosen, the selected device having conveniently low f_T. Certain physical data was available for this device with which derived parameters could be compared. The results reported in the present section are restricted to the study of this single device sample and should be regarded as a test of the feasibility of the procedure of parameter evaluation, rather than an exhaustive assessment of its applicability and accuracy.

IV.1 The Basic Measurements

The theory of Section II assumes an idealized device with exponential base grading; although the grading for the type 2N696 undoubtedly deviates from this ideal (particularly near the emitter), the theory is applied in the following, the transistor being regarded as represented by an "exponential model". The basic measurements necessary are of τ' ($= 1/\omega_T$) as a function of emitter current at constant collector voltage, and of change of transit time τ and fractional collector capacitance C_c with change of collector voltage at constant emitter current. The results of these measurements, carried out at 1 mc/s, are given in Figures 5 through 7, respectively. Parameters are evaluated for $V_c = 5$ v, $I_e = -0.2$ ma.

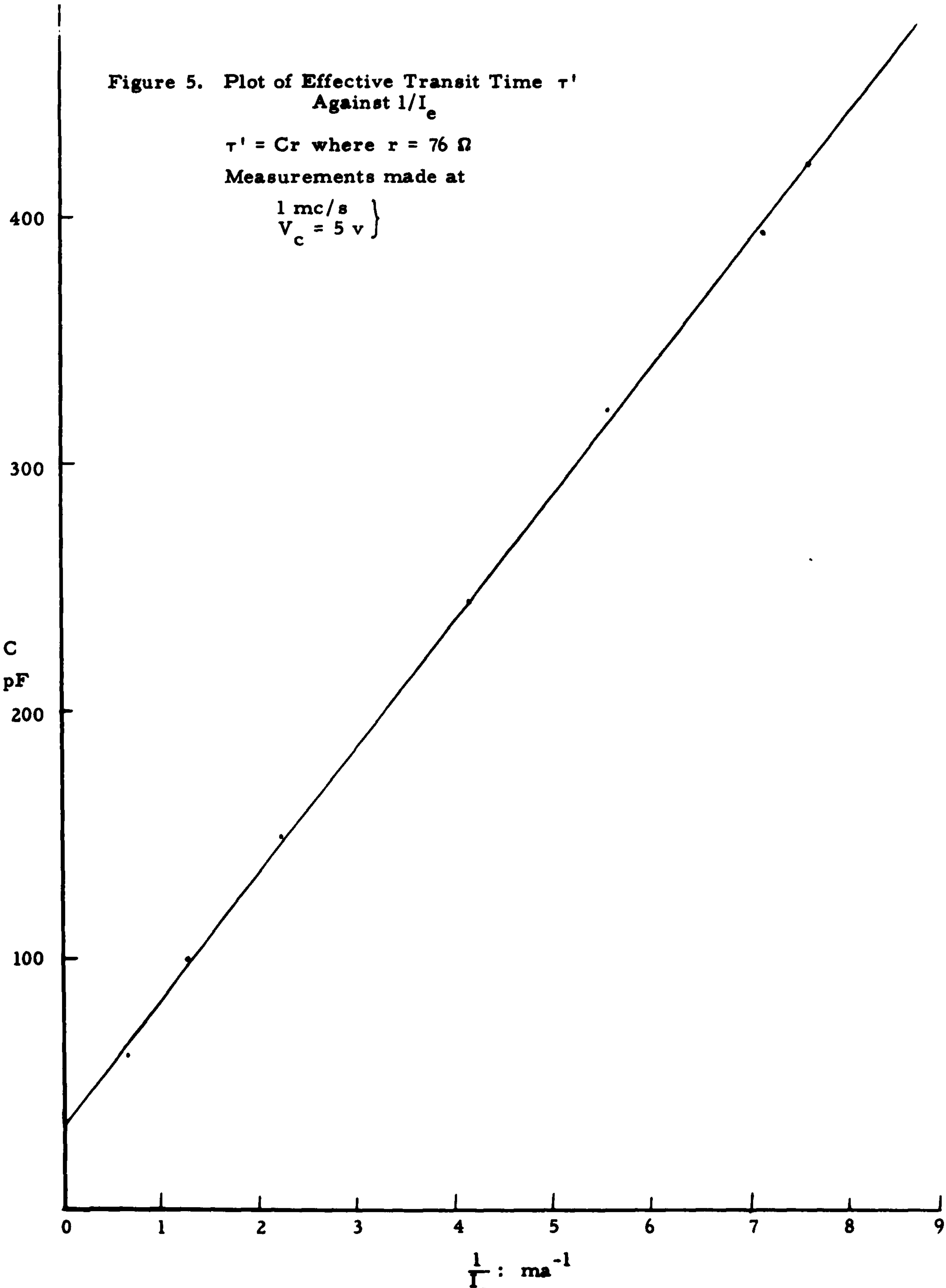

Figure 5. Plot of Effective Transit Time τ' Against $1/I_e$

$\tau' = Cr$ where $r = 76\ \Omega$

Measurements made at

$\left.\begin{array}{l} 1\ mc/s \\ V_c = 5\ v \end{array}\right\}$

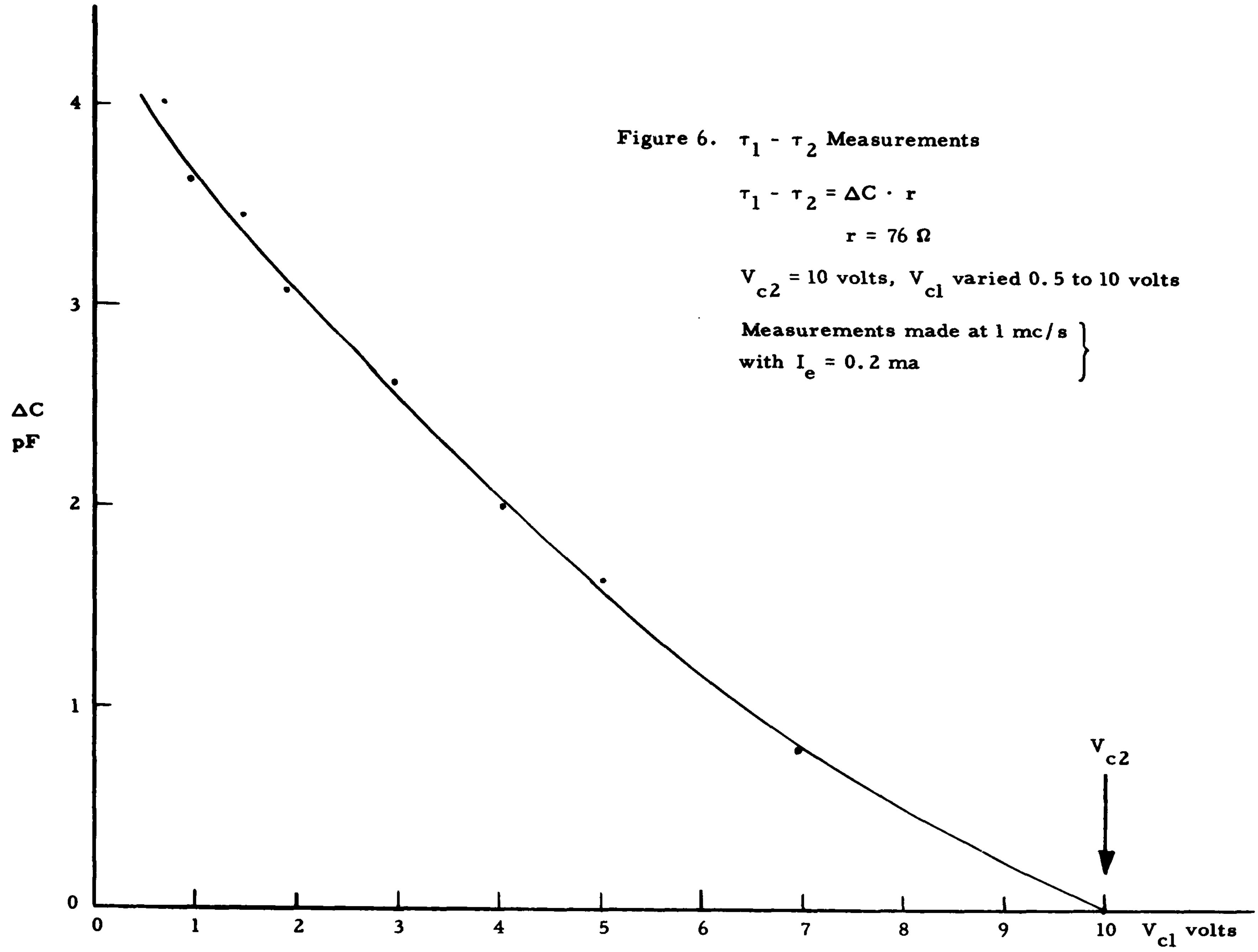

Figure 6. $\tau_1 - \tau_2$ Measurements

$\tau_1 - \tau_2 = \Delta C \cdot r$

$r = 76\ \Omega$

$V_{c2} = 10$ volts, V_{c1} varied 0.5 to 10 volts

Measurements made at 1 mc/s with $I_e = 0.2$ ma

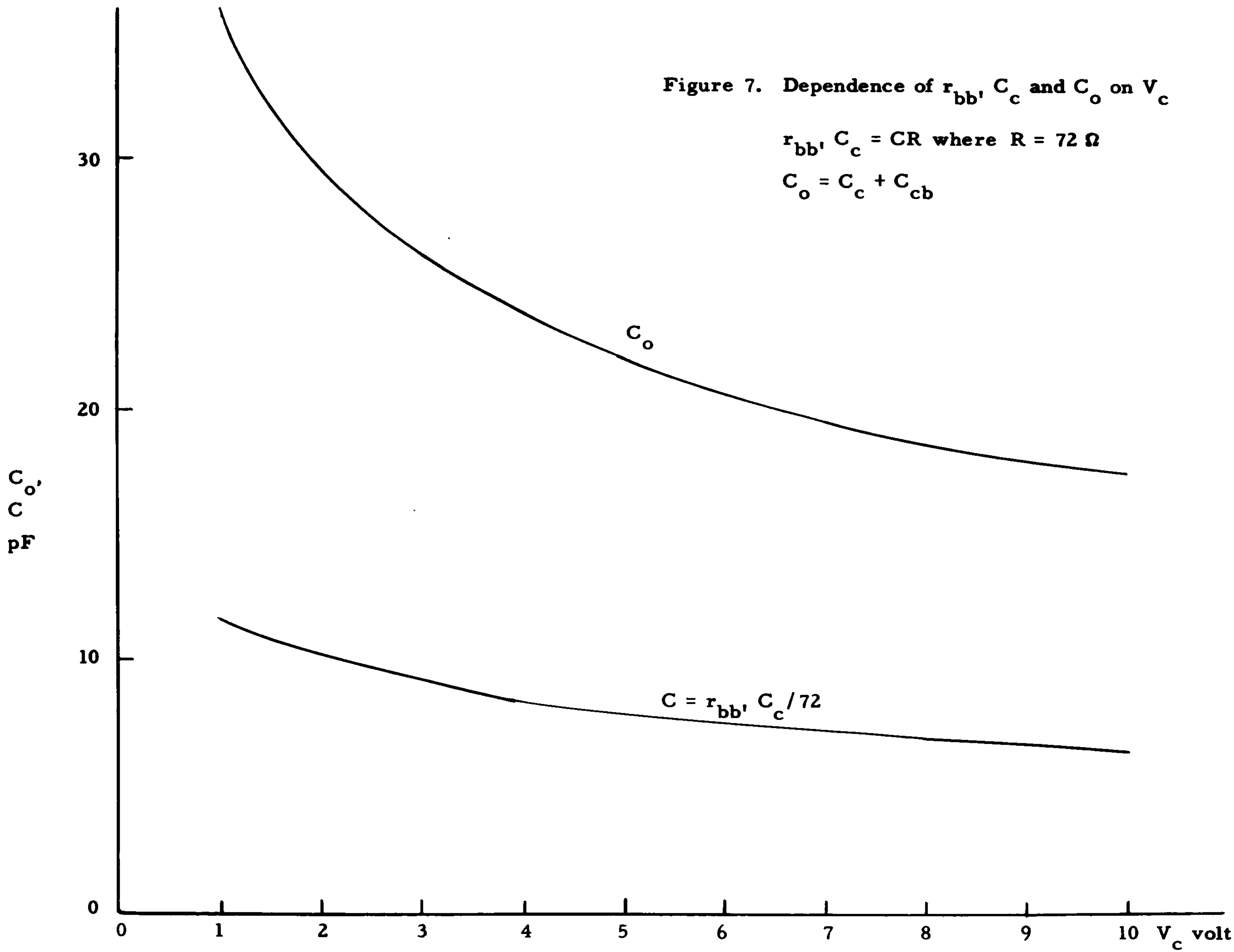

Figure 7. Dependence of $r_{bb'}$ C_c and C_o on V_c

$r_{bb'} C_c = CR$ where $R = 72\ \Omega$

$C_o = C_c + C_{cb}$

From the plot of τ' against $1/I_e$ in Figure 5 one obtains:

$\tau = 2.36 \times 10^{-9}$ secs

$f_\tau = 1/2\pi\ \tau = 67.5$ mc/s

and $C_{te} + C_{ob} = 150$ pF

from the slope of the line. Also, for $I_e = -5.0$ ma, $V_c = 5$ v

$\tau' = 3.2 \times 10^{-9}$ secs

$f_T = 1/2\pi\ \tau' = 50$ mc/s

In Figure 6 the difference in transit time with collector voltage change with respect to $V_c = 10$ v is plotted. From these results, in conjunction with ratios of $r_{bb'} C_c$ products derived from Figure 7, $\tau_1 - \tau_2$ is plotted as a function of ln (C_{c1}/C_{c2}) in Figure 8. It is seen that a straight line relationship is obtained for collector voltages down to 3 v: this suggests that the assumed theory is applicable and the transistor approximates reasonably to the exponential model.

Also plotted in Figure 8 are points derived from common-base open-current output capacitance measurements. Neglecting stray capacitance between transistor leads, the output capacitance

$$C_{ob} = C_c + C_{cb}$$

and is the total collector depletion capacitance. Thus C_{ob} may be expected to behave with change of V_c in the same manner as does C_c; this is seen to be the case, the latter points agreeing quite well with those derived from the $r_{bb'} C_c$ data.

From equation (12) the slope of the above straight line plot is L^2/D, giving for $V_c = 5$ v,

$$L = 1.3 \times 10^{-4} \text{ cm}$$

From equations (15) the values of the field factor and base width are

$m = 5.35$

$w = 6.95 \times 10^{-4}$ cm.

However, these values are accurate only if the ratio d/L is sufficiently large at the collector voltages considered for the approximation $F \simeq 1$ in equations (10) and (14) to be made.

Figure 8. Relationship Between $\tau_1 - \tau_2$ and $\ln (C_{c1}/C_{c2})$

• : by measurement of $r_{bb'}$, C_c ratios

× : by measurement of C_o ratios

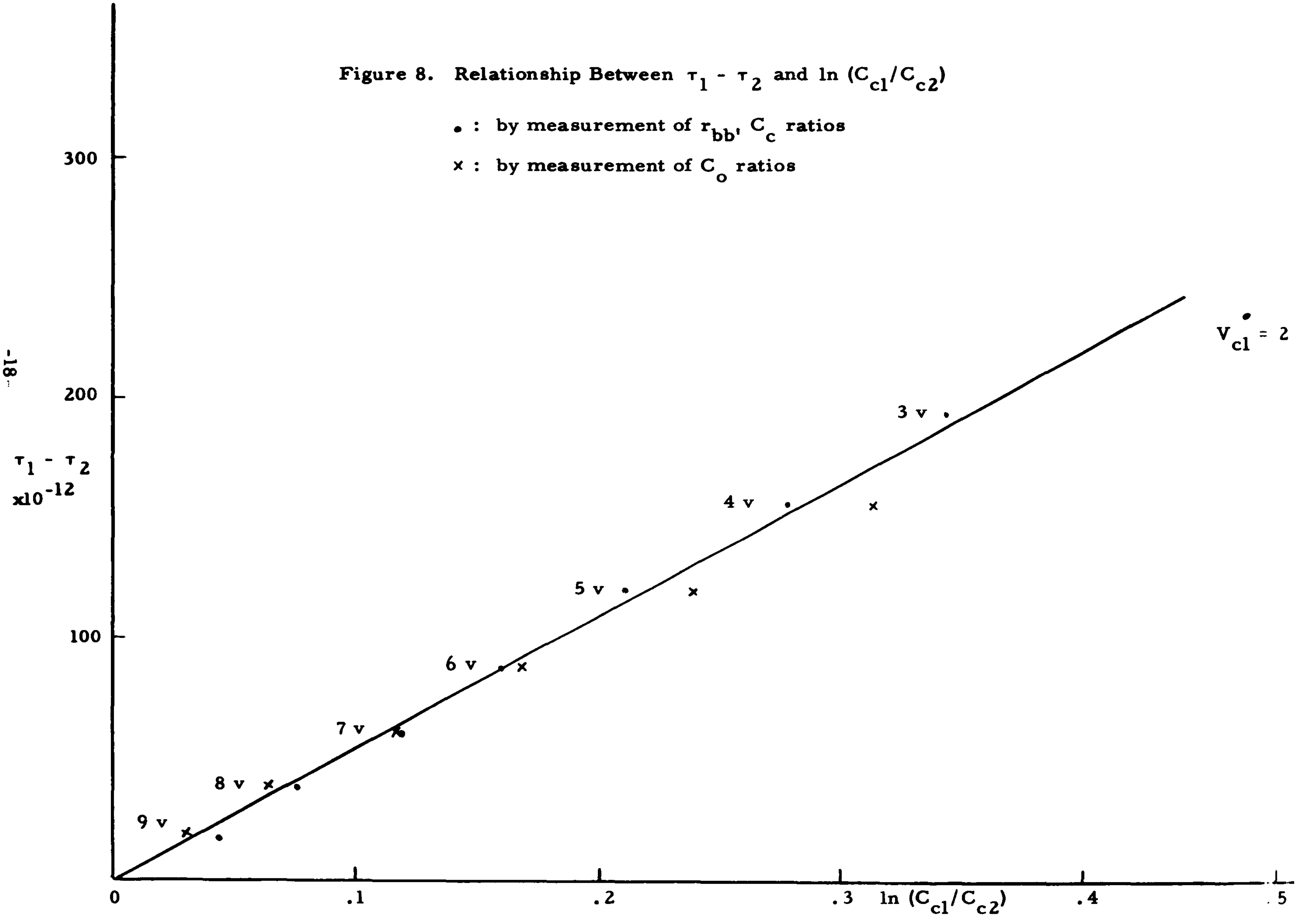

IV.2 Other Measurements

In order to evaluate the ratio d/L and verify the above calculations it is necessary to determine the emitter area A_e and the collector capacitance C_c for the collector voltage concerned. Then

$$C_c = \kappa A_e/d$$

Figure 9 gives measurements of $1/C_{te}^2$ as a function of reverse emitter-base voltage. For voltages greater than 2 v a straight line relationship is exhibited, indicating approximate step junction behavior. From the slope of this straight line, according to equation (17)

$$N_1 A_e^2 = 8.84 \times 10^{10} \text{ cm}$$

The d.c. relationship between I_c and V_{eb}, plotted in Figure 10, is a straight line, the slope of which gives

$$\frac{A_e}{N_1} = .643 \times 10^{-20} \text{ cm}^5$$

It is noted from equation (18) that this last quantity is proportional to L, the above derived value of which has been used at this stage. If the value of L is later found to be in error owing to $F \neq 1$, the A_e/N_1 ratio needs to be modified when solution by iteration is applied as discussed in Section II.3. Thus

$$A_e^3 = .569 \times 10^{-9} \text{ cm}^6$$

and

$$A_e = .83 \times 10^{-3} \text{ cm}.$$

The $r_{bb'} C_c$ product at $V_c = 5$ v is seen from Figure 7 to be

$$r_{bb'} C_c = .57 \times 10^{-9} \text{ sec}$$

Thus it now remains to determine $r_{bb'}$ so that C_c and hence d may be calculated. The procedure of Section III.3, carried out at 1 mc/s with $V_c = 5$ v and $I_e = 0.2$ ma, yields

$$r_{bb'} = 625 - 476 = 149\ \Omega$$

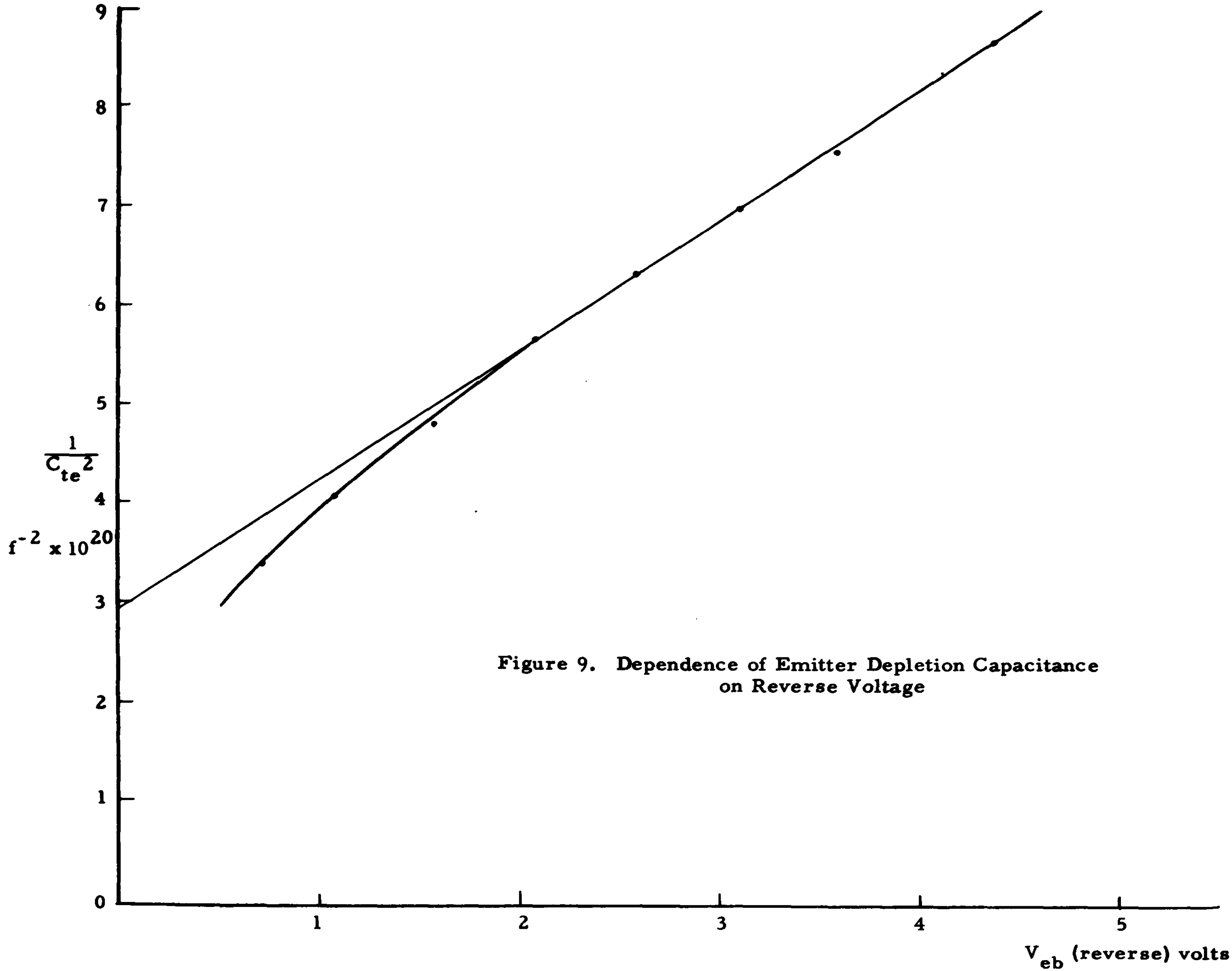

Figure 9. Dependence of Emitter Depletion Capacitance on Reverse Voltage

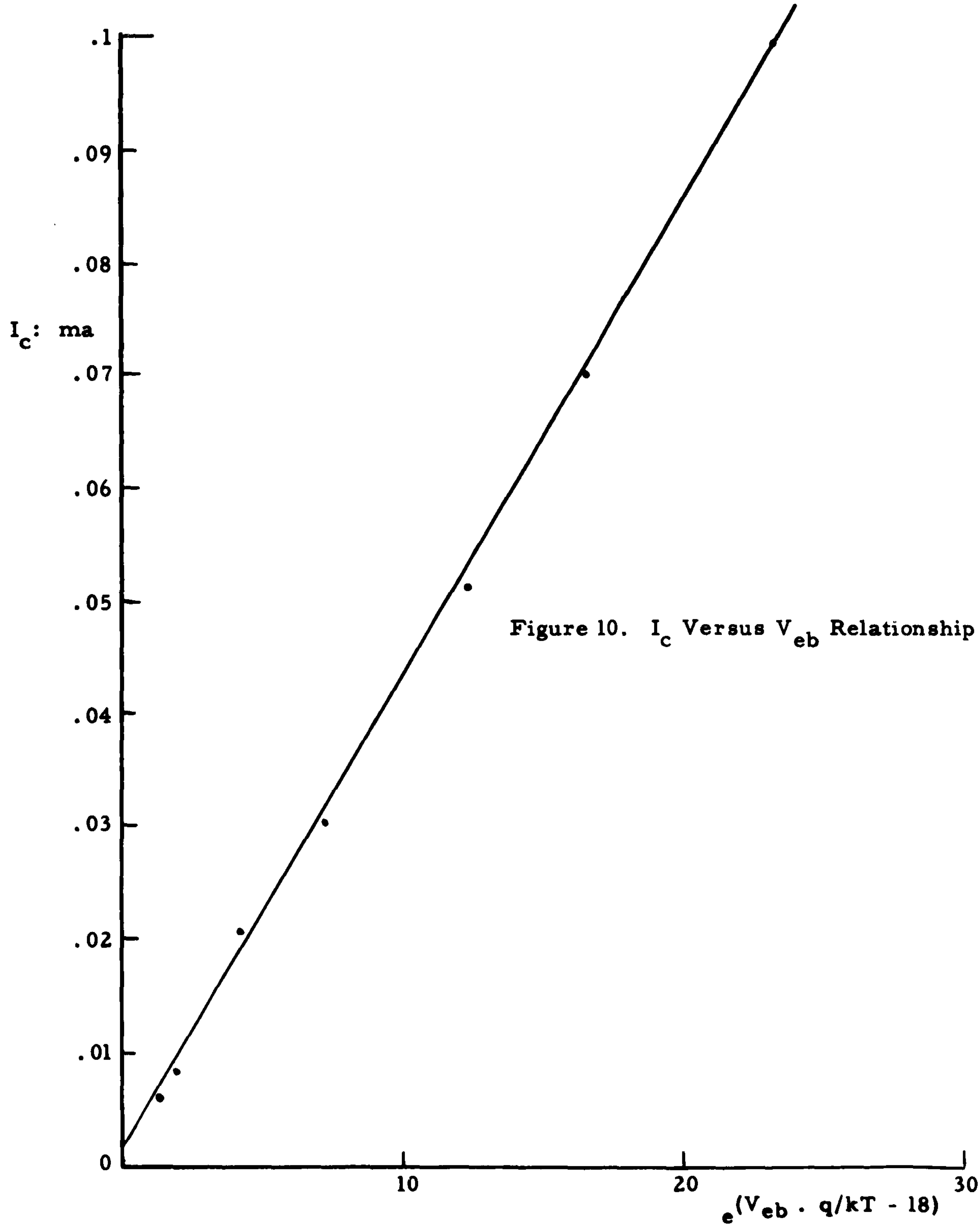

Figure 10. I_c Versus V_{eb} Relationship

Details of this derivation are given in Appendix III.

$$\therefore \qquad C_c = 3.8 \text{ pF}$$

and

$$d = 2.33 \times 10^{-4}$$

Hence $\dfrac{d}{L} = 1.79$

and this value is insufficiently large for the approximation $F \simeq 1$ to be valid. Iteration must therefore be applied to determine the true value of L.

IV.3 <u>Iteration Process</u>

For the purpose of determining L by iteration, the collector voltages

$$V_{c1} = 3 \text{ v}$$

$$V_{c2} = 10 \text{ v}$$

were used for which, on the basis of $L = 1.3 \times 10^{-4}$ cm as above,

$$d_1 = 2.0 \times 10^{-4} \text{ cm}, \qquad \frac{d_1}{L} = 1.54$$

$$d_2 = 2.87 \times 10^{-4} \text{ cm}, \qquad \frac{d_2}{L} = 2.21$$

yielding

$$F = 1.13$$

Evaluating the modified value of L from equation (14) gives

$$L = 1.58 \times 10^{-4}$$

and results in change of A_e to

$$A_e = .883 \times 10^{-3} \text{ cm}^2$$

After recalculating d_1 and d_2 for this modified A_e,

$$\left.\begin{aligned} d_1/L &= 1.35 \\ d_2/L &= 1.93 \\ F &= 1.156 \\ \text{and} \quad L &= 1.65 \times 10^{-4} \text{ cm} \end{aligned}\right\}$$

Finally, using this last L value,

$$\left.\begin{aligned} A_e &= .896 \times 10^{-3}\ \text{cm} \\ d_1/L &= 1.31 \\ d_2/L &= 1.88 \\ F &= 1.16 \\ L &= 1.67 \times 10^{-4}\ \text{cm} \end{aligned}\right\}$$

A further iteration results in negligible change in parameter values.

IV.4 Summary of Derived Parameter Values

Having determined values of L and d to satisfy equation (9), it is possible to calculate all parameters discussed in Section II. The final results of these calculations are given below:

$V_c = 5$ v

$L = 1.67 \times 10^{-4}$ cm
$m = 3.64$
$w = 6.08 \times 10^{-4}$ cm

$A_e = 0.896 \times 10^{-3}\ \text{cm}^2$
$D_e = 338 \times 10^{-4}$ cm (emitter diameter)

$d = 2.51 \times 10^{-4}$ cm
$d/L = 1.505$

$N_1 = 1.09 \times 10^{17}\ \text{cm}^{-3}$
$N_2 = 1.47 \times 10^{15}\ \text{cm}^{-3}$
$N_1/N_2 = 73.6$

$w_b = 7.18 \times 10^{-4}$ cm

$\tau = 2.36 \times 10^{-9}$ secs; $f_\tau = 67.5$ mc/s
$C_{ob} = 22.2$ pF
$C_c = 3.8$ pF
$C_{cb} = 18.4$ pF

$C_{te} = 128\ \text{pF}^{+}$

$r_{bb'} C_c = 0.57 \times 10^{-9}$ secs

$r_{bb'} = 150\ \Omega$

V. DISCUSSION

In the previous section, theory based on a device model with exponential base grading has been applied somewhat blindly to a double-diffused n-p-n silicon unit. The results derived may be regarded as referring to an equivalent exponential model of the actual transistor studied. Just how close the physical parameters obtained (e.g., base width, emitter area, depletion layer thickness) are to the corresponding quantities in the device can only be established by carrying out more detailed investigations.

Because of the diffused nature of the emitter junction (rather than the assumed step junction of Section II) it might be expected that marked divergence from the theoretical relationships of Section II would be observed during the course of the measurements. However, the relationship between $\tau_1 - \tau_2$ and $\ln C_{c1}/C_{c2}$ (Figure 8) is quite as predicted by theory, suggesting that deviations from exponential grading are not severe.

The plot of $1/C_{te}^{\,2}$ against reverse V_e in Figure 9 indicates the gradual, rather than step nature of the emitter junction, the linear relationship being exhibited only for voltages greater than 2 v. Since for forward biasing of the emitter junction the depletion layer must, in view of the behavior of Figure 9, fall short of the region of highest impurity density in the base, the interpretation of the $I_c \sim V_{eb}$ data of Figure 10 in terms of the expression of equation (18) is of uncertain significance. Again, provided that deviations from the assumed ideal device are not serious, use of this expression should presumably give the N_1 value of an approximating exponential impurity density distribution.

It is interesting to compare derived physical parameters with device design data given by the manufacturer, as below:

$^{+}$Derived from the slope $(C_{te} + C_{ob})\, r_d$ of the plot of τ' against $1/I_e$ in Figure 5.

	Device design value	From measurements
D_e	375×10^{-4} cm	338×10^{-4} cm
N_1	1.4×10^{17} cm^{-3}	1.1×10^{17} cm^{-3}
N_2	2.5×10^{15}	1.5×10^{15} cm^{-3}

In view of the approximations made in applying the theory to the 2N696 unit, the agreement is remarkably good.

The extrinsic base resistance value listed in Section IV.4 would perhaps seem to be somewhat large for the type of transistor studied, and needs to be verified by other methods of measurement[4]. From the relative area of the emitter and collector as specified by the manufacturer (namely 1:4) a value of 5 pF would seem reasonable for C_c; from the measured $r_{bb'} C_c$ value of 0.57×10^{-9} secs, the corresponding $r_{bb'}$ value would be 114 Ω. If this value is used in the calculations of Section IV, then $L = 1.93 \times 10^{-4}$ cm, $D_e = 346 \times 10^{-4}$ cm and $N_1 = 1.24 \times 10^{17}$ cm^{-3}.

VI. CONCLUSIONS

A possible approach to the derivation of physical parameters of drift transistors having a diffused collector junction has been presented on the basis of an exponentially graded base model. The measurements involved are all relatively simple and are carried out at quite low frequencies--i.e., frequencies of the order of f_β. No difficulty has been experienced in practice in performing the measurements involved with sufficient accuracy for their interpretation in analytic terms, provided that the theory is assumed valid for the device concerned.

Detailed studies have been made of a type 2N696 n-p-n silicon mesa unit. Although the base impurity density is known to depart appreciably from an exponential distribution, owing to the double-diffused process of fabrication, the results obtained appear to conform reasonably well to the exponential theory, certain of the derived physical parameters being quite close to the manufacturer's design values for the device.

More investigation is required before the true significance of physical parameters derived by the procedure presented in the report can be assessed. For some devices a complementary error function, or perhaps Gaussian, distribution of infinite density may be appropriate. The same general analytic procedure could be applied in such cases, though with greater complexity.

APPENDIX I. DETAILS OF THE TRANSIT TIME BRIDGE

The circuit of the bridge used for the measurements of Section IV is given in Figure 11. For satisfactory operation a compact layout is necessary, care being taken to reduce stray effects and coupling between emitter, base and collector circuit meshes to a minimum. The arrangement adopted consisted of four screened compartments, within which were:

base circuit elements C, R
collector path through r to ground
emitter excitation lead-in
detector transformer.

Interconnections between these screened boxes were kept as short as possible, with complete separation of emitter excitation and output detector transformer.

The variable capacitors C_1, C_2 were small vane-type with spindles and moving vanes grounded. R was an Allen-Bradley carbon track potentiometer with the moving contact grounded: this arrangement gave consistent calibrations of resistance over a long time period, while the stray capacitance was found to be ~ 2 pF and constant over the full range of resistance (this capacitance was also constant over the frequency range 0.5 to 5 mc/s, for which the bridge was designed and operated).

Particular care is necessary in the design of the detector transformer which converts out-of-balance voltage between collector and base to a voltage with respect to ground. The two windings need to be reasonably efficiently coupled magnetically yet screened from each other electrostatically. The construction adopted was to have the two halves of a 1/2" D.

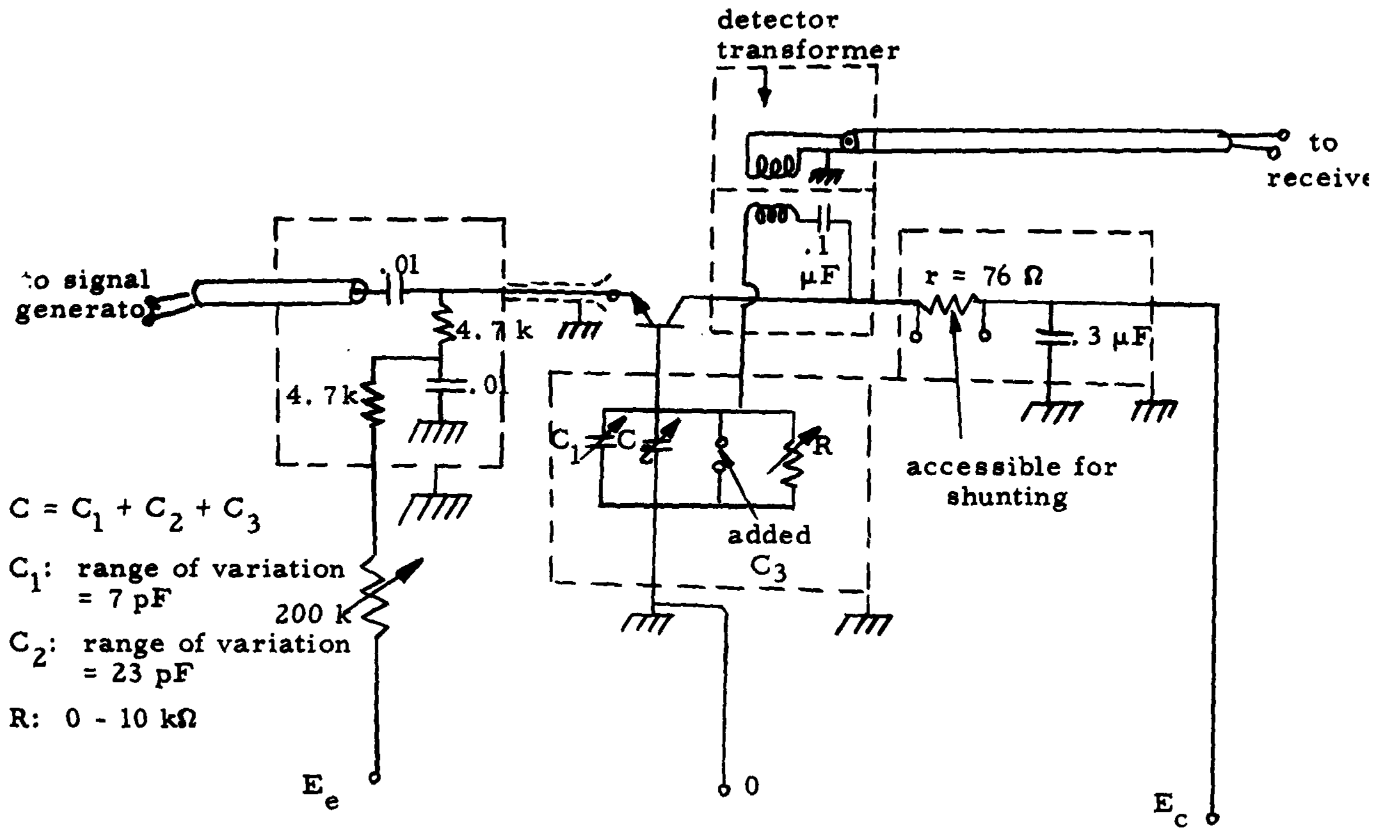

a) Circuit layout

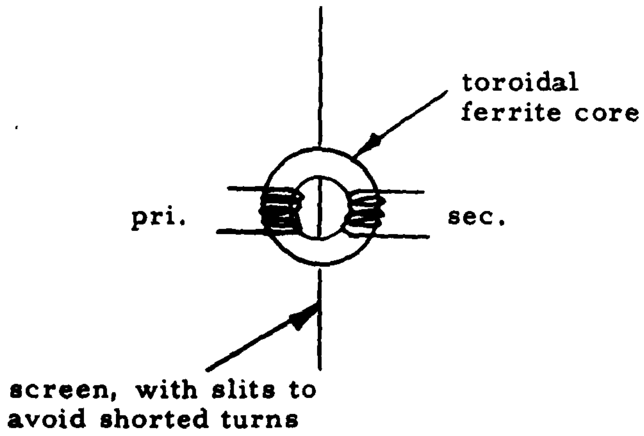

b) Preferred design of detector transformer

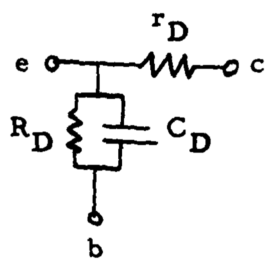

c) "Transistor dummy" used for calibration of the bridge

Figure 11. Details of Bridge for Measurement of Effective Transit Time on ω_T

ferrite por-core assembly, containing the respective windings, separated by a thin (.006") grounded copper screening sheet (with appropriate slit): this gave excellent shielding but the distributed capacitance of the windings to ground was necessarily rather large (of the order of 10 pF). A better construction is as shown in Figure 11b, the two windings being on opposite extremes of a ferrite toroidal core and well separated from the screening sheet. A 1/2" D. toroid is very suitable for the purpose.

The bridge was constructed specifically for carrying out the measurements reported, but should have other features incorporated if employed generally for measurement of effective transit time τ' or f_T. A single variable capacitor, possibly of range 10 - 60 pF is adequate provided other fixed capacitors can be switched in to give a sufficiently large range of the capacitance C (for example, capacitance steps of 50 pF up to 500 pF). While using the bridge it was necessary on occasions to reduce r by adding shunting resistors. This facility is best incorporated into the design of the bridge, means being provided for plugging or switching in shunting elements, without introducing undue lead strays. A useful minimum value of r is 10 Ω.

Bridge elements R and C were calibrated by direct admittance bridge measurements at the base terminal of the transistor socket, and by using the transit time bridge to measure the (known) elements R_D, C_D of the "transistor dummy" shown in Figure 11c.

APPENDIX II. DETAILS OF THE BRIDGE ARRANGEMENT FOR MEASUREMENT OF $r_{bb'}$, C_c

Figure 12 gives the circuit details of the jig used for measurement of $r_{bb'}$, C_c, in conjunction with the Wayne Kerr admittance bridge. The variable capacitor C was of moving vane type giving a range of 6 to 16 pF. Care was necessary to avoid stray capacitance effects associated with the circuit CR; for this reason the element C was mounted in a screening can. Calibration of C was carried out with the Wayne Kerr bridge by regarding the capacitor as a three-terminal element with respect to ground. Of the stray capacitances C_1, C_2 only the latter is significant in the operation of the bridge and the reactance of this is negligibly high in comparison with the resistance R for the frequencies concerned ($\leq$ 5 mc/s).

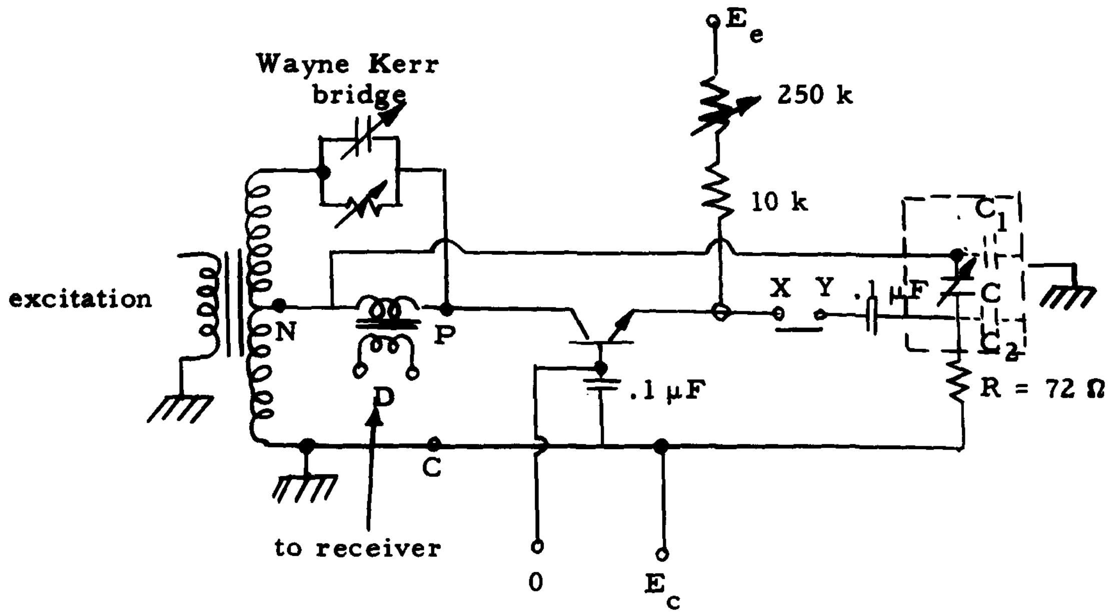

Figure 12. Circuit Arrangement of Figure Used for Measurement of $r_{bb'}$ C_c and C_o

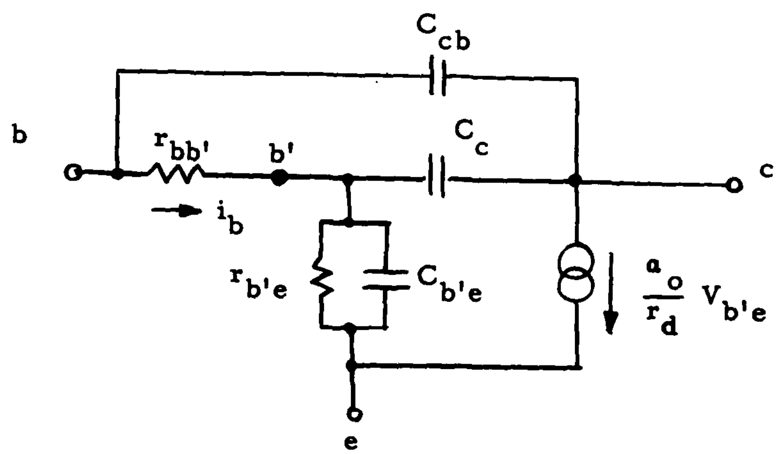

Figure 13. Equivalent Circuit of the Transistor Assumed in Determination of $r_{bb'}$

APPENDIX III. DETERMINATION OF $r_{bb'}$ OF 2N696 SAMPLE STUDIED IN SECTION IV

Measurements made at 1 mc/s with $V_c = 5$ v, $I_e = -0.2$ ma gave

$$\tau' = 21.8 \times 10^{-9} \text{ sec}$$

$$\beta_o = 12$$

Assuming that in regard to the effects of C_{cb} on τ', $r_{bb'}$ may be neglected,

$$\tau' \simeq \tau + r_d (C_{te} + C_c + C_{cb})$$

Thus, representing the transistor by the equivalent circuit of Figure 13,

$$C_c + C_{b'e} \approx \tau' r_d - C_{cb} = 150 \text{ pF}$$

$$r_{b'e} = r_d/(1 - \alpha_o) = 1695\ \Omega$$

The impedance seen to the right of b'e, with collector started to emitter, may be written

$$r_1 + jx_1 = 1/y_{b'e}$$

where

$$r_1 = r_{b'e}/\left\{1 + r_{b'e}^{\ 2}\, \omega^2 (C_c + C_{b'e})^2\right\}$$

$$= 476\ \Omega$$

Now if the short-circuit base input admittance of the transistor in common emitter configuration is written

$$y_{11} = y_{11}' + j\omega C_{cb} = \frac{1}{R_{be}} + j\omega C_{be}$$

and $\quad 1/y_{11}' = r_2 + jx_2$

then $\quad r_{bb'} \approx r_2 - r_1$

Measurement of y_{11} gives

$$R_{be} = 1570\ \Omega$$

$$C_{be} = 142.5 \text{ pF}$$

$\therefore \quad C_{b'e} = C_{be} - C_{cb} = 124.5$ pF

and $\quad r_2 = 625\ \Omega$

giving

$$r_{bb'} = 149\ \Omega$$

REFERENCES

1. Das, M. B. and Boothroyd, A. R., "Determination of Physical Parameters of Diffusion and Drift Transistors," Trans. IRE on Electron Devices, ED-8, No. 1 (January 1961), pp. 15-30.
2. Das, M. B. and Boothroyd, A. R., "Impurity Density Distribution in the Base Region of Drift Transistors," to appear in Trans. IRE on Electron Devices, (November 1961).
3. Turner, R. J., "Surface Barrier Transistors, Measurements and Applications," Tele-Tech., 13 (1954), p. 78.
4. Das, M. B., "On the Determination of the Extrinsic Equivalent Circuit Parameters of Drift Transistors," Journal of Electronics and Control, Vol. 8, No. 5 (May 1960).

DISTRIBUTION LIST
AF 49(638)-1043

ORGANIZATION	NO. COPIES
Advanced Research Projects Agency Washington 25, D. C.	1
Aeronautical Research Laboratories Attn: Technical Library, Bldg. 450 Wright-Patterson Air Force Base Ohio	1
Applied Mechanics Reviews Southwest Research Institute 8500 Culebra Road San Antonio 6, Texas	1
ARO, Inc. Attn: AEDC Library Arnold Air Force Station Tullahoma, Tennessee	1
ASTIA Attn: TIPCR Arlington Hall Station Arlington 12, Virginia	10
Prof. N. Bloembergen Department of Physics Harvard University Cambridge 38, Massachusetts	1
Prof. Harvey Brooks Department of Physics Harvard University Cambridge 38, Massachusetts	1
Chairman, Canadian Joint Staff For DRB/DSIS 2450 Massachusetts Ave., N.W. Washington 25, D. C.	1
Chief, Physics Branch Division of Research U.S. Atomic Energy Commission Washington 25, D. C.	1
Commandant Air Force Institute of Technology (AU) Library, MCLI-LIB, Bldg. 125, Area B Wright-Patterson Air Force Base Ohio	1
Commander Air Force Cambridge Research Laboratories Attn: CRREL L. G. Hanscom Field Bedford, Massachusetts	1
Commander Air Force Flight Test Center Attn: FTOTL Edwards Air Force Base California	1
Commander Air Force Missile Development Center Attn: HDOI Holloman Air Force Base New Mexico	1
Commander Air Force Office of Scientific Research Attn: SRY Washington 25, D. C.	3
Commander Air Force Research Division Attn: RRRTL Washington 25, D. C.	2
Commander Air Force Special Weapons Center Attn: SWOI Kirtland Air Force Base New Mexico	1
Commander Air Research and Development Command Attn: RDR Andrews Air Force Base Washington 25, D. C.	2
Commander Air Research and Development Command Attn: RDRA Andrews Air Force Base Washington 25, D. C.	1
Commander Air Research and Development Command Attn: RDRB Andrews Air Force Base Washington 25, D. C.	1
Commander Air Research and Development Command Attn: RDRC Andrews Air Force Base Washington 25, D. C.	1
Commander Air Research and Development Command Attn: RDRS Andrews Air Force Base Washington 25, D. C.	1
Commander Army Rocket and Guided Missile Agency Attn: ORDXR OTL Redstone Arsenal Alabama	
Commander, Detachment 1 Hq. Air Force Research Division The Shell Building Brussels, Belgium	2
Commander Rome Air Development Center Attn: RAYLD Griffiss Air Force Base Rome, New York	1
Commander Wright Air Development Division Attn: WWAD Wright-Patterson Air Force Base Ohio	4
Commanding General U.S. Army Signal Corps Research and Development Laboratory Attn: SIGFM/EL-RPO Fort Monmouth, New Jersey	1
Director, Army Research Office Attn: Scientific Information Branch Department of the Army Washington 25, D. C.	1
Director, Department of Commerce Office of Technical Services Washington 25, D. C.	1
Director, Naval Research Laboratory Attn: Technical Information Officer Washington 25, D. C.	1
Director, Office of Ordnance Research Box CM, Duke Station Durham, North Carolina	1
Director of Research and Development Headquarters, USAF Attn: AFDRD Washington 25, D. C.	1
General Electric Company Electron Tube Division of the Research Laboratory The Knolls Schenectady, New York Attn: E. D. McArthur	1
Dr. Harold Glaser Office of Naval Research Washington 25, D. C.	1
Harvard University Cruft Laboratory Cambridge 38, Massachusetts Attn: Technical Reports Collection	1
Hughes Aircraft Company Florence at Teale St. Culver City, California Attn: Documents Group, Bldg. 6, Rm. X2015	1
Institute of Aeronautical Sciences Attn: Librarian 2 East 64 St. New York 16, New York	1
Prof. Zohrab Kaprielian University of Southern California School of Engineering Department of Electrical Engineering University Park Los Angeles 7, California	1
Prof. P. Kusch Department of Physics Columbia University New York 2, New York	1
Massachusetts Institute of Technology Research Laboratories of Electronics Room 20B-221, Document Office Cambridge 39, Massachusetts Attn: J. H. Hewitt	1
Hans Motz Oxford University Oxford, England	1
National Aeronautics and Space Administration Washington 25, D. C.	6
National Bureau of Standards Library Room 203, Northwest Building Washington 25, D. C.	1
Office of Naval Research Department of the Navy Attn: Code 420 Washington 25, D. C.	1
Ohio State University Department of Electrical Engineering Columbus, Ohio	1
Mr. F. Okress Sperry Gyroscope Company Electron Tube Division Mail Station 1B40 Great Neck, New York	
Physics Program National Science Foundation Washington 25, D. C.	1
P.O. Box AA Wright-Patterson Air Force Base Ohio	1
RCA Laboratories Princeton, New Jersey Attn: Dr. W. M. Webster, Director Electronics Research Laboratories	1
Dr. Irving Rowe Office of Naval Research 346 Broadway New York, New York	1
Sylvania Electric Company Mountain View, California Attn: D. H. Goodman	1
Technical Information Libraries Bell Telephone Laboratories, Inc. Whippany Laboratory Whippany, New Jersey Attn: Technical Reports Librarian	1
Prof. Charles Townes Department of Physics Columbia University New York 27, New York	1
University of Illinois Department of Electrical Engineering Urbana, Illinois Attn: H. Von Foerster	1
The University of Michigan Department of Electrical Engineering Electron Physics Laboratory Ann Arbor, Michigan Attn: Prof. J. E. Rowe	1
U.S. Atomic Energy Commission Technical Information Extension P.O. Box 62 Oak Ridge, Tennessee	1
Varian Associates 611 Hansen Way Palo Alto, California Attn: Technical Library	1
Westinghouse Electric Corp. Electronic Tube Division P.O. Box 284 Elmira, New York Attn: Mr. Sheldon S. King, Librarian	1
M. D. Adcock, Head Microwave Systems and Components American Systems, Inc. 3412 Century Boulevard Inglewood, California	1
Antenna Laboratory Electrical Engineering Research Laboratory University of Illinois Urbana, Illinois Attn: Dr. P. F. Mayes	1
Antenna Laboratory Ohio State University Research Foundation Columbus, Ohio Attn: Dr. C. T. Tai	1
Assistant Secretary of Defense Research and Development Board Department of Defense Washington 25, D. C.	1
Bell Telephone Laboratories, Inc. Central Serial Records Technical Information Library 463 West St. New York 14, New York	1
Boeing Aircraft Company Physical Research Unit Seattle 14, Washington Attn: Mr. R. W. Tilman	1
Dr. C. J. Bouwkamp Phillip's Research Laboratories N. V. Phillip's Gloeilampenfabrieken Eindhoven, Netherlands VIA ONR London	1
Brooklyn Polytechnic Institute Microwave Research Institute 55 Johnson St. Brooklyn 1, New York Attn: Dr. A. Oliner	1
California Institute of Technology Pasadena, California Attn: C. H. Papas	1
Cambridge University Radiophysics Division Cavendish Laboratory Cambridge, England VIA ONR London Attn: Mr. J. A. Ratcliffe	1
Chalmers Institute of Technology Goteborg, Sweden VIA ONR London Attn: Prof. S. Ekelof and Prof. H. Wallman	
Chief, Bureau of Aeronautics Navy Department Washington 25, D. C. Attn: EL-51	1
Chief, Bureau of Ships Navy Department Washington 25, D. C. Attn: Code 838	2
Chief of Naval Research Navy Department Washington 25, D. C. Attn: Code 427	2
Chief of Naval Research Navy Department Washington 25, D. C. Attn: Code 460	1
Commander Air Force Office of Scientific Research Air Research and Development Command Washington 25, D. C.	1
Columbia Radiation Laboratories Columbia University 538 W. 120th St. New York 27, New York Attn: Librarian	1
Commander Naval Air Development Center Johnsville, Pennsylvania Attn: AEEL	1
Commander U.S. Naval Electronics Laboratory San Diego, California	1
Commanding General Rome Air Development Center Griffiss Air Force Base Rome, New York Attn: RCRW	1
Commanding General Signal Corps Engineering Laboratories Evans Signal Laboratory Area Building 27 Belmar, New Jersey Attn: Technical Documents Center	1
Commanding General Signal Corps Engineering Laboratories Fort Monmouth, New Jersey Attn: SIGEL-SMB-ml, MO8-Magnetic Materials	1
Commanding General Wright Air Development Center Wright Patterson Air Force Base Ohio Attn: WCRKO 2	1
Commanding Officer Squier Signal Laboratory Fort Monmouth, New Jersey Attn: V. J. Kublin	1
Prof. N. DeClaris Cornell University Ithaca, New York	1
Department of Electrical Engineering Cornell University Ithaca, New York Attn: Dr. H. G. Booker	1
Department of Electrical Engineering Yale University New Haven, Connecticut	1
Director, Naval Research Laboratory Washington 25, D. C. Attn: Code 2000	1
Director, Naval Ordnance Laboratory White Oak, Maryland	1
Director, Naval Research Laboratory Washington 25, D. C. Attn: Code 5250	1
Douglas Aircraft Co., Inc. El Segundo Division El Segundo, California	1
Electrical Engineering Department Illinois Institute of Technology Technology Center Chicago 16, Illinois	1
Electrical Engineering Department University of Texas Box F, University Station Austin, Texas	1
Electronics Research Laboratory Stanford University Stanford, California Attn: Applied Electronics Laboratory Documents Library	1
Federal Telecommunications Laboratories, Inc. 500 Washington Ave. Nutley, New Jersey Attn: A. K. Wing	1

ORGANIZATION	NO. COPIES
Georgia Institute of Technology Atlanta, Georgia Attn: Mrs. J. Fenley Crosland, Librarian	1
Carl A. Hedberg, Head Electronics Division Denver Research Institute University of Denver Denver, Colorado	1
Hughes Aircraft Company Antenna Research Department Bldg. 12, Room 2617 Culver City, California	1
Hughes Aircraft Company Research and Development Library Culver City, California Attn: John T. Milek	1
Library Boulder Laboratories National Bureau of Standards Boulder, Colorado Attn: Victoria S. Barker	2
Mathematics Research Group New York University 25 Waverly Place New York, New York Attn: Dr. M. Kline	1
Mr. Frank J. Mullin Department of Electrical Engineering California Institute of Technology Pasadena, California	1
Naval Air Missile Test Center Point Mugu, California	1
Office of the Chief Signal Officer Pentagon Washington 25, D. C. Attn: SIGET	1
Office of Technical Services Department of Commerce Washington 25, D. C.	1
Radiation Laboratory Johns Hopkins University 1315 St. Paul St. Baltimore 2, Maryland Attn: Librarian	1
The Rand Corporation 1700 Main St. Santa Monica, California Attn: Margaret Anderson, Librarian	1
Randall Morgan Laboratory of Physics University of Pennsylvania Philadelphia 4, Pennsylvania	1
Regents of the University of Michigan Ann Arbor, Michigan	1
Research Laboratory of Electronics Document Room Massachusetts Institute of Technology Cambridge 39, Massachusetts Attn: Mr. J. Hewitt	1
Prof. Vincent C. Rideout Department of Electrical Engineering University of Wisconsin Madison 6, Wisconsin	1
Royal Technical University Laboratory for Telephony and Telegraphy Oestervoldgade 10 Copenhagen, Denmark VIA ONR London Attn. Prof. H. L. Knudsen	1
Prof. Samuel Seely, Head Department of Electrical Engineering Case Institute of Technology University Circle Cleveland 6, Ohio	1
Signal Corps Engineering Laboratories Fort Monmouth, New Jersey Attn Mr. O. C. Woodyard	1
Stanford Research Institute 974 Commercial Stanford, California Attn: Dr John T. Bolljohn Division of Electrical Engineering	1
Technical Reports Collection 303A Pierce Hall Harvard University Cambridge 38, Massachusetts	1

ORGANIZATION	NO. COPIES
Technical University Department of Electrical Engineering Delft, Holland VIA ONR London Attn: Prof. J. P. Schouten	1
University of Florida Gainesville, Florida Attn: Applied Electronics Laboratory Document Library	1
U.S. Naval Post Graduate School Monterey, California Attn: Librarian	1
Watson Laboratories Library AMC, Red Bank, New Jersey Attn: ENAGSI	1
Willow Run Research Center University of Michigan Ypsilanti, Michigan Attn: Dr. K. Siegel	1
Advisory Group on Electron Tubes 346 Broadway New York 13, New York	2
Bell Telephone Laboratories Murray Hill, New Jersey Attn: Dr. W. Kluver	1
California Institute of Technology Electron Tube and Microwave Laboratory Pasadena, California Attn: Prof. R. Gould	1
Chief, Bureau of Ships Department of the Navy Washington 25, D. C. Attn: 691A4	1
Chief of Ordnance Washington 25, D. C. Attn: ORDTX-AR	1
Chief of Research and Development OCS, Department of the Army Washington 25, D. C.	1
Chief Signal Officer Department of the Army Washington 25, D. C. Attn: SIGRD	1
Chief, U.S. Army Security Agency Arlington Hall Station Arlington 12, Virginia	2
Commander Air Force Command and Control Development Division Air Research and Development Command United States Air Force Laurence G. Hanscom Field Bedford, Massachusetts Attn: CROTL	1
Commander Wright Air Development Division Attn: WCOSI-3 Wright-Patterson Air Force Base Ohio	2
Commanding Officer Diamond Ordnance Fuze Laboratories Washington 25, D. C. Attn: Library, Rm. 211, Bldg. 92	1
Commanding Officer Frankford Arsenal Philadelphia 37, Pennsylvania Attn: ORDBA-FEL	1
Commanding Officer and Director U.S. Navy Electronics Laboratory San Diego 52, California	1
Commanding Officer, 9560th TSU U.S. Army Signal Electronics Research Unit P.O. Box 205 Mountain View, California	1
Commanding Officer U.S. Army Signal Material Support Agency Attn: SIGMS-ADJ	1
Commanding Officer U.S. Army Signal Research and Development Laboratory Fort Monmouth, New Jersey Attn Director of Research	1
Commanding Officer Office of Naval Research, Branch Office 1000 Geary St. San Francisco 9, California	1

ORGANIZATION	NO. COPIES
Commanding Officer U.S. Army Signal Research and Development Laboratory Fort Monmouth, New Jersey Attn: Technical Documents Center	1
Commanding Officer U.S. Army Signal Research and Development Laboratory Fort Monmouth, New Jersey Attn: SIGRA/SL-PRM (Records File Copy)	1
Commanding Officer U.S. Army Signal Research and Development Laboratory Fort Monmouth, New Jersey Attn: Logistics Division (For SIGRA/SL-PRM) (Project Engineer)	2
Commanding Officer U.S. Army Signal Research and Development Laboratory Fort Monmouth, New Jersey Attn: Technical Information Division (FOR RETRANSMITTAL TO ACCREDITED BRITISH AND CANADIAN GOVERNMENT REPRESENTATIVES AND TO DEPARTMENT OF COMMERCE)	5
Deputy President U.S. Army Security Agency Board Arlington Hall Station Arlington 12, Virginia	1
Director, U.S. Naval Research Laboratory Washington 25, D. C. Attn: Code 2027	1
The European Office U.S. Army R and D Liaison Group APO 757 New York, New York (FOR RETRANSMITTAL TO CONTRACTOR, DA 91-591-EUC-1312)	1
Hughes Aircraft Company Culver City, California Attn: Dr. Mendel, Microwave Tube Laboratory	1
Marine Corps Liaison Office U.S. Army Signal Research and Development Laboratory Fort Monmouth, New Jersey	1
Massachusetts Institute of Technology Research Laboratory of Electronics Cambridge, Massachusetts Attn: Prof. L. Smullin	1
OASD (R and E), Rm. 3E1065 The Pentagon Washington 25, D. C. Attn: Technical Library	1
Radio Corporation of America Laboratories Princeton, New Jersey Attn: Dr. L. S. Nergaard	1
Raytheon Manufacturing Company Microwave and Power Tube Operations Waltham 54, Massachusetts Attn: W. C. Brown	1
Research Division Library Raytheon Company 28 Seyon St. Waltham 54, Massachusetts	1
S.F.D. Laboratories, Inc. 800 Rahway Ave. Union, New Jersey	1
Stanford University Electronic Research Laboratory Palo Alto, California Attn: Prof. D. A. Watkins	1
Sylvania Electric Products Physics Laboratory Bayside, Long Island, New York Attn: L. R. Bloom	1
U.S. Navy Electronics Liaison Office U.S. Army Signal Research and Development Laboratories Fort Monmouth, New Jersey	1
Watkins-Johnson Company 333 Hillview Ave. Stanford Industrial Park Palo Alto, California	1
Westinghouse Electric Corporation Research Laboratory Beulah Road, Churchill Boro Pittsburgh 35, Pennsylvania	1